AIAA JOURNAL
Vol. 46, No. 4, April 2008

Improvement of Flügge's Equations for Buckling of Moderately Thick Anisotropic Cylindrical Shells

Atsushi Takano*
Mitsubishi Electric Corporation, Kanagawa 247-8520, Japan

DOI: 10.2514/1.31277

A theoretical analysis of the buckling problems of anisotropic laminated or sandwich, short or long, circular cylindrical shells under axial loads is presented. The theory is based on Flügge's equations, improved by using first-order shear deformation theory. Nonlinear partial differential equations of equilibrium and boundary conditions are obtained by using a strain of finite displacement theory and the principle of virtual work, and these nonlinear partial differential equations of equilibrium are linearized. Solutions that satisfy the partial differential equations of equilibrium and boundary condition are obtained, and the analytical model is verified by presenting some numerical results and comparing them with results from previous studies.

Nomenclature

A_{ij}	=	in-plane stiffness
A^*_{ij}	=	$1/a_{ij}$
$[a]$	=	$[A]^{-1}$, in-plane compliance
B_{ij}	=	extensional/flexural coupling
D_{ij}	=	flexural stiffness
$e_{\lambda\mu}$	=	Green's strain tensor in local rectangular Cartesian coordinates
$f_{\lambda\mu}$	=	Green's strain tensor in general curvilinear coordinates
G_{ij}	=	transverse shear modulus
K_c	=	normalized axial load factor
k_{ij}	=	shear correction factor
l	=	length of the cylindrical shell
M_x, M_θ, $M_{\theta x}$, $M_{x\theta}$	=	moment resultants per unit length
m	=	number of half-waves in the axial direction
N_x, N_θ, $N_{\theta x}$, $N_{x\theta}$	=	in-plane force resultants per unit length
n	=	number of waves in circumferential direction
P	=	external axial compression per unit length
q_2, q_3	=	load parameter
R	=	radial coordinate
r	=	radius of the cylindrical shell
S_{ij}	=	transverse shear stiffness
T	=	external torsional force per unit length
t	=	thickness of the cylindrical shell
U, V, W, Γ_x, Γ_θ	=	amplitude of the displacements
$\mathcal{U}$, $\mathcal{V}$, $\mathcal{W}$	=	displacement field in the x, θ, and z directions
u, v, w	=	middle surface displacements in the x, θ, and z directions
v^λ, v_λ	=	contravariant and covariant components of the displacement vector
$v^\lambda_{;\mu}$, $v_{\lambda;\mu}$	=	covariant derivative of v^λ and v_λ
x	=	axial coordinate of the middle surface
y^1, y^2, y^3	=	Cartesian coordinates
z	=	radial coordinate of the middle surface
α^1, α^2, α^3	=	curvilinear coordinate
γ_x, γ_θ	=	rotation of lines normal to the middle surface
ε_x, ε_θ, $\gamma_{x\theta}$, γ_{xz}, $\gamma_{\theta z}$	=	strain components
θ	=	circumferential coordinate of the middle surface
ν, ν_1, ν_2	=	Poisson's ratio
Π	=	total potential energy
σ_x, σ_θ, $\tau_{x\theta}$	=	stress components

Subscripts

x, θ, z	=	derivatives with respect to the x, θ, and z directions
0	=	forces or displacements in the prebuckling state.

Superscript

$*$	=	increments of forces or displacements upon buckling

I. Introduction

BECAUSE aircraft and satellites are getting larger every year, so are the thin and moderately thick circular cylindrical shells made of laminated or honeycomb-sandwich carbon-fiber-reinforced plastic (CFRP) that are important structural parts of aircraft and satellites. The many studies analyzing the buckling of orthotropic or anisotropic circular cylindrical shells that have been reported in the past few decades [1–7] cannot be applied to long circular cylindrical shells such as a strut or the central cylinder of a satellite or the fuselage of aircraft, because they are based on Donnell's theory [8], which is a shallow-shell-theory approximation. A buckling analysis based on deep-shell theory is needed.

Cheng and Ho [9,10] extended Flügge's buckling theory, which is one of the deep-shell theories, to the buckling of anisotropic circular cylindrical shells under combined axial, radial, and torsional loads. Bert and Kim [11] applied Cheng and Ho's [9,10] theory to the torsional buckling of hollow laminated-composite drive shafts, but that theory is based on the classical laminate theory in which the transverse shear deformation of the shell is ignored. When it is applied to a laminated or honeycomb-sandwich circular cylindrical shell, the predicted buckling load might be too large because the transverse shear deformation of these shells is not negligible.

Stein and Mayers [12] obtained a simple solution for the axial buckling of an orthotropic circular cylindrical shell, and their solution included the effect of transverse shear deformation. Their solution, however, is also based on Donnell's theory [8] and thus cannot be applied to long circular cylindrical shells.

Geier and Singh [13] and Resse and Bert [14] presented analyses of the buckling of a laminated circular cylindrical shell that were

Received 28 March 2007; accepted for publication 19 November 2007.

*Engineer, Mechanical Engineering Section, Space Systems Department, Kamakura Works, 325 Kamimachiya, Kamakura; Takano.Atsushi@dr.MitsubishiElectric.co.jp

based on deep-shell theory and that took transverse shear deformation into account. Kardomateas and Philobos [15] derived a three-dimensional theory of elasticity for the buckling of an orthotropic circular cylindrical thick or thin shell under combined axial compression and external pressure. But these two analyses and this theory ignore coupling stiffness.

The purpose of the work reported in the present paper was to develop a method for predicting the buckling load of anisotropic, laminated or sandwich, long or short, circular cylindrical shells under axial loads. Torsional force is also considered so that this method can be extended in the future.

This paper derives an analytical model for anisotropic circular cylindrical shells that is based on deep-shell theory, including first-order shear deformation theory. Deep-shell theories have been proposed by Love [16], Timoshenko and Gere [17], Sanders [18], and Flügge [19]. Flügge's theory is the least simplified of those theories, and so this paper extends Flügge's equations and derives buckling equations for moderately thick anisotropic circular cylindrical shells. A solution that satisfies the boundary condition is obtained, and some numerical examples are presented for validation.

The solution is based on linear bifurcation theory and thus does not include the effect of shape imperfection. But laminated circular cylindrical shells and honeycomb-sandwich circular cylindrical shells with laminated skins are made by using mandrels. The mandrel shape is generally highly accurate, and that accuracy is reflected in the circular cylindrical shells. Thus, these shells have only small shape imperfections and the solution is useful for designing these shells.

II. Basic Relations and Hypotheses

Consider a circular cylindrical shell of thickness t, radius r, and length l that is made of a laminate consisting of N orthotropic layers of uniform thickness bonded together perfectly. Axial compression per unit length P and torsional (shearing) force per unit length T are applied to the circular cylindrical shell. The coordinate system and notations are shown in Fig. 1.

The following assumptions concerning shell motions are made:

1) Strains are very small when compared with unity.

2) Lines that are straight and normal to the middle surface before deformation remain straight during deformation but not necessarily normal to the middle surface (first-order shear deformation theory).

3) Changes of curvature are assumed to be sufficiently small to allow linearization of curvatures.

4) The prebuckling state is assumed to be axisymmetric displacement and membrane stress.

5) Transverse normal stress σ_z and normal strain ε_z are smaller than other stress and strain components.

III. Derivation of Equations

For the purpose of developing a theory that takes the transverse shear deformation effects into account for moderately thick shells, the following displacement field is assumed (as shown in Fig. 2):

$$\begin{aligned}
&\mathcal{U}(x,\theta,z) \equiv u - z(w_{,x} - \gamma_x)\\
&\mathcal{V}(x,\theta,z) \equiv v - z(w_{,\theta}/r - \gamma_\theta - v/r)\\
&\mathcal{W}(x,\theta,z) \equiv w
\end{aligned} \tag{1}$$

Green's strain tensor $f_{\lambda\mu}$ in general curvilinear coordinates $(\alpha^1,\alpha^2,\alpha^3)$ is defined as follows [20]:

$$f_{\lambda\mu} = \tfrac{1}{2}(v_{\lambda;\mu} + v_{\mu;\lambda} + v_{\kappa;\lambda}v^{\kappa}_{;\mu}) \qquad (\lambda,\mu,\kappa = 1,2,3) \tag{2}$$

where

$$(v_1,v_2,v_3) = (\mathcal{W},\mathcal{V}/R,\mathcal{U}), \qquad (\alpha^1,\alpha^2,\alpha^3) = (R,\theta,x) \tag{3}$$

and repeated Greek subindices imply summations.

This strain tensor $f_{\lambda\mu}$ can be transformed into the strain tensor $e_{\lambda\mu}$ in the local rectangular Cartesian coordinates y^1, y^2, and y^3 as follows [20]:

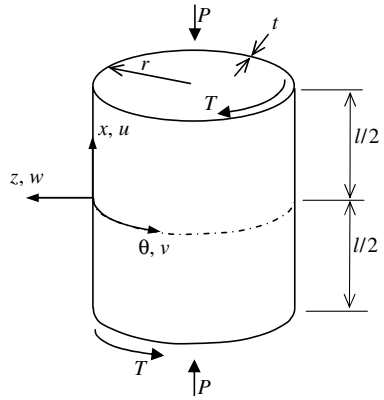

Fig. 1 Shell geometry and notations.

$$e_{\lambda\mu} = \frac{\partial\alpha^{\kappa}}{\partial y^{\lambda}}\frac{\partial\alpha^{\rho}}{\partial y^{\mu}} f_{\kappa\rho} \qquad (\lambda,\mu,\kappa,\rho = 1,2,3) \tag{4}$$

where

$$(y^1,y^2,y^3) = (R,R\theta,x) \tag{5}$$

Substituting Eq. (2) into Eq. (4) and rewriting R as $r+z$, we can express the strains in terms of $\mathcal{U}$, $\mathcal{V}$, and $\mathcal{W}$ as follows:

$$\begin{aligned}
\varepsilon_x &= \mathcal{U}_{,x} + \frac{1}{2}\{(\mathcal{U}_{,x})^2 + (\mathcal{V}_{,x})^2 + (\mathcal{W}_{,x})^2\}\\
\varepsilon_\theta &= \frac{r}{r+z}\frac{\mathcal{V}_{,\theta}}{r} + \frac{1}{r+z}\mathcal{W}\\
&\quad + \frac{1}{2}\left(\frac{r}{r+z}\right)^2\left\{\left(\frac{\mathcal{U}_{,\theta}}{r}\right)^2 + \left(\frac{\mathcal{V}_{,\theta}}{r} + \frac{\mathcal{W}}{r}\right)^2 + \left(\frac{\mathcal{W}_{,\theta}}{r} - \frac{\mathcal{V}}{r}\right)^2\right\}\\
\gamma_{x\theta} &= \mathcal{V}_{,x} + \frac{r}{r+z}\frac{\mathcal{U}_{,\theta}}{r}\\
&\quad + \left(\frac{r}{r+z}\right)\left\{\mathcal{U}_{,x}\frac{\mathcal{U}_{,\theta}}{r} + \frac{\mathcal{V}_{,x}}{r}(\mathcal{V}_{,\theta} + \mathcal{W}) + \frac{\mathcal{W}_{,x}}{r}(\mathcal{W}_{,\theta} - \mathcal{V})\right\}\\
\gamma_{xz} &= \gamma_x\\
\gamma_{z\theta} &= \frac{r}{r+z}\gamma_\theta \cong \gamma_\theta
\end{aligned} \tag{6}$$

where

$$\varepsilon_x = e_{33}, \quad \varepsilon_\theta = e_{22}, \quad \gamma_{x\theta} = 2e_{23}, \quad \gamma_{xz} = 2e_{13}, \quad \gamma_{z\theta} = 2e_{12} \tag{7}$$

and because of assumption 5,

$$\varepsilon_z \equiv 0 \tag{8}$$

When transverse shear deformation is taken into account, the stress-strain relations of anisotropic material are

$$\begin{bmatrix}\sigma_x\\ \sigma_\theta\\ \tau_{x\theta}\end{bmatrix} = \begin{bmatrix}E_{11} & E_{12} & E_{16}\\ E_{12} & E_{22} & E_{26}\\ E_{16} & E_{26} & E_{66}\end{bmatrix}\begin{bmatrix}\varepsilon_x\\ \varepsilon_\theta\\ \gamma_{x\theta}\end{bmatrix}$$
$$\begin{bmatrix}\tau_{xz}\\ \tau_{\theta z}\end{bmatrix} = \begin{bmatrix}G_{11} & G_{12}\\ G_{12} & G_{22}\end{bmatrix}\begin{bmatrix}\gamma_{xz}\\ \gamma_{\theta z}\end{bmatrix} \tag{9}$$

With these coefficients given, the resultant force (moment) and stress relations of moderately thick shell elements can be written as

$$\{N_x, N_{x\theta}, M_x, M_{x\theta}\} = \int_{-t/2}^{t/2} \{\sigma_x, \tau_{x\theta}, \sigma_x z, \tau_{x\theta} z\}\left(1+\frac{z}{r}\right)\mathrm{d}z$$
$$\{N_{\theta x}, N_\theta, M_{\theta x}, M_\theta\} = \int_{-t/2}^{t/2} \{\tau_{x\theta}, \sigma_\theta, \tau_{x\theta} z, \sigma_\theta z\}\,\mathrm{d}z \tag{10}$$
$$Q_{xz} = \int_{-t/2}^{t/2} \tau_{xz}\left(1+\frac{z}{r}\right)\mathrm{d}z \cong \int_{-t/2}^{t/2} \tau_{xz}\,\mathrm{d}z \qquad Q_{\theta z} = \int_{-t/2}^{t/2} \tau_{\theta z}\,\mathrm{d}z$$

Equilibrium conditions are obtained from the principle of virtual work. The total potential energy Π is given by

$$\Pi = \frac{1}{2}\int_{-l/2}^{l/2}\int_0^{2\pi}\int_{-t/2}^{t/2} (\sigma_x\varepsilon_x + \sigma_\theta\varepsilon_\theta + \tau_{x\theta}\gamma_{x\theta} + \tau_{xz}\gamma_{xz} + \tau_{\theta z}\gamma_{\theta z})\left(1+\frac{z}{r}\right)\mathrm{d}z r\mathrm{d}\theta\,\mathrm{d}x - \int_0^{2\pi}[-Pu - Tv]_{x=-l/2}^{x=l/2} r\,\mathrm{d}\theta \tag{11}$$

The equilibrium equations are obtained by setting the total virtual work equal to zero,

$$\delta\Pi = 0 \tag{12}$$

yielding the following five nonlinear partial differential equations as Euler–Lagrange equations:

$$\begin{aligned}
&N_{x,x} + N_{\theta x,\theta}/r + (N_x u_{,x})_{,x} + N_{\theta x,x} u_{,\theta}/r + N_{\theta x,\theta} u_{,x}/r \\
&\quad + 2N_{\theta x} u_{,x\theta}/r + (N_\theta u_{,\theta})_{,\theta}/r^2 = 0 \\
&N_{x\theta,x} + M_{\theta,\theta}/r^2 + N_{\theta,\theta}/r + M_{x\theta,x}/r + (N_x v_{,x})_{,x} + N_{x\theta,x} v_{,\theta}/r \\
&\quad + N_{x\theta,\theta} v_{,x}/r + 2N_{x\theta}(v_{,x\theta} + w_{,x})/r + N_{\theta x,x} w/r \\
&\quad + (N_\theta v_{,\theta})_{,\theta}/r^2 + N_{\theta,\theta} w_{,\theta}/r + 2N_\theta w_{,\theta}/r - N_\theta v/r^2 = 0 \\
&M_{x,xx} + M_{x\theta,x\theta}/r + M_{\theta x,x\theta}/r + M_{\theta,\theta\theta}/r^2 - N_\theta/r + (N_x w_{,x})_{,x} \\
&\quad + N_{\theta x,x} w_{,\theta}/r + N_{\theta x,\theta} w_{,x}/r - 2N_{x\theta} v_{,x}/r + 2N_{\theta x} w_{,x\theta}/r \\
&\quad - N_{x\theta,x} v/r - 2N_\theta v_{,\theta}/r^2 - N_\theta w/r^2 \\
&\quad + (N_\theta w_{,\theta})_{,\theta}/r^2 - N_{\theta,\theta} v/r^2 = 0 \\
&M_{x,x} + M_{\theta x,\theta}/r - Q_{xz} = 0 \\
&M_{\theta,\theta}/r + M_{x\theta,x} - Q_{\theta z} = 0
\end{aligned} \tag{13}$$

and the boundary conditions are specified by

$$\begin{aligned}
&\delta u = 0 \quad \text{or} \quad N_x + N_x u_{,x} + N_{\theta x} u_{,\theta}/r = -P \\
&\delta v = 0 \quad \text{or} \quad N_{x\theta} - M_{x\theta}/r + N_x v_{,x} \\
&\qquad\qquad + N_{\theta x}(v_{,\theta} + w)/r = -T \\
&\delta w = 0 \quad \text{or} \quad M_{x,x} + (M_{\theta x,\theta} + M_{x\theta,\theta})/r + N_x w_{,x} \\
&\qquad\qquad + N_{\theta x} w_{,\theta}/r - N_{x\theta} v/r = 0 \\
&\delta(w_{,x} - \gamma_{xz}) = 0 \quad \text{or} \quad M_x = 0 \\
&\delta\gamma_{\theta z} = 0 \quad \text{or} \quad M_{x\theta} = 0
\end{aligned} \tag{14}$$

at $x = -l/2$ and $l/2$.

To obtain the linearized equilibrium equations for the buckling of circular cylindrical shells, we let

$$\begin{aligned}
&u = u_0 + u^*, \qquad v = v_0 + v^*, \qquad w = w_0 + w^* \\
&N_x = N_{x0} + N_x^*, \qquad N_{\theta x} = N_{\theta x0} + N_{\theta x}^* \quad \cdots \quad N_\theta = N_\theta^*
\end{aligned} \tag{15}$$

Substituting Eqs. (15) into Eqs. (13) and (14) and considering the prebuckling uniform axisymmetric state and neglecting all products of increments yields the following five linearized partial differential equations and boundary conditions:

$$\begin{aligned}
&N_{x,x} + N_{\theta x,\theta}/r - Pu_{,xx} - 2Tu_{,x\theta}/r = 0 \\
&N_{x\theta,x} + M_{\theta,\theta}/r^2 + N_{\theta,\theta}/r + M_{x\theta,x}/r \\
&\quad - Pv_{,xx} - 2T(v_{,x\theta} + w_{,x})/r = 0 \\
&M_{x,xx} + M_{x\theta,x\theta}/r + M_{\theta x,x\theta}/r + M_{\theta,\theta\theta}/r^2 \\
&\quad - N_\theta/r - Pw_{,xx} - 2T(-v_{,x} + w_{,x\theta})/r = 0 \\
&M_{x,x} + M_{\theta x,\theta}/r - Q_{xz} = 0 \\
&M_{\theta,\theta}/r + M_{x\theta,x} - Q_{\theta z} = 0
\end{aligned} \tag{16}$$

$$\begin{aligned}
&\delta u = 0 \quad \text{or} \quad N_x = 0 \\
&\delta v = 0 \quad \text{or} \quad N_{x\theta} - M_{x\theta}/r = 0 \\
&\delta w = 0 \quad \text{or} \quad M_{x,x} + (M_{\theta x,\theta} + M_{x\theta,\theta})/r = 0 \\
&\delta(w_{,x} - \gamma_{xz}) = 0 \quad \text{or} \quad M_x = 0 \\
&\delta\gamma_{\theta z} = 0 \quad \text{or} \quad M_{x\theta} = 0
\end{aligned} \tag{17}$$

In Eqs. (16) and (17), increment displacements and forces u^*, N_x^*, etc., are rewritten as u, N_x, etc., for convenience.

Equations (16) and (17) can be expressed in terms of increments of the displacements. Substituting Eqs. (1) into Eqs. (6) and neglecting $(z/r)^3$ or higher orders yields the following strain and displacement relations:

$$\begin{aligned}
\varepsilon_x &= u_{,x} - z(w_{,xx} - \gamma_{x,x}) \\
\varepsilon_\theta &= \frac{v_{,\theta}}{r} + \frac{w}{r} - \frac{z}{r}\left(\frac{w_{,\theta\theta}}{r} - \gamma_{\theta,\theta} + \frac{w}{r}\right) + \left(\frac{z}{r}\right)^2\left(\frac{w_{,\theta\theta}}{r} - \gamma_{\theta,\theta} + \frac{w}{r}\right) \\
\gamma_{x\theta} &= v_{,x} + \frac{u_{,\theta}}{r} - \frac{z}{r}\left(\frac{u_{,\theta}}{r} - v_{,x} + 2w_{,x\theta} - r\gamma_{\theta,x} - \gamma_{x,\theta}\right) \\
&\quad + \left(\frac{z}{r}\right)^2\left(\frac{u_{,\theta}}{r} + w_{,x\theta} - \gamma_{x,\theta}\right) \\
\gamma_{xz} &= \gamma_x \\
\gamma_{\theta z} &= \gamma_\theta
\end{aligned} \tag{18}$$

Substituting Eqs. (9) and (18) into Eqs. (10) and neglecting $(z/r)^3$ or higher orders yields the corresponding resultant force (moment) and displacement relations.

For example, N_x, M_x, and $M_{x\theta}$ are

$$\begin{aligned}
N_x &= \int_{-t/2}^{t/2} \sigma_x\left(1+\frac{z}{r}\right)\mathrm{d}z \\
&= \int_{-t/2}^{t/2} (E_{11}\varepsilon_x + E_{12}\varepsilon_\theta + E_{16}\gamma_{x\theta})\left(1+\frac{z}{r}\right)\mathrm{d}z \\
&= \int_{-t/2}^{t/2}\Bigg[E_{11}\left(1+\frac{z}{r}\right)\{u_{,x} - z(w_{,xx} - \gamma_{x,x})\} \\
&\quad + E_{12}\left(1+\frac{z}{r}\right)\left\{\frac{v_{,\theta}}{r} + \frac{w}{r} - \frac{z}{r}\left(\frac{w_{,\theta\theta}}{r} - \gamma_{\theta,\theta} + \frac{w}{r}\right) + \left(\frac{z}{r}\right)^2\left(\frac{w_{,\theta\theta}}{r} - \gamma_{\theta,\theta} + \frac{w}{r}\right)\right\} \\
&\quad + E_{16}\left(1+\frac{z}{r}\right)\left\{v_{,x} + \frac{u_{,\theta}}{r} - \frac{z}{r}\left(\frac{u_{,\theta}}{r} - v_{,x} + 2w_{,x\theta} - r\gamma_{\theta,x} - \gamma_{x,\theta}\right) + \left(\frac{z}{r}\right)^2\left(\frac{u_{,\theta}}{r} + w_{,x\theta} - \gamma_{x,\theta}\right)\right\}\Bigg]\mathrm{d}z \\
&= A_{11}u_{,x} + A_{12}\left(\frac{v_{,\theta}}{r} + \frac{w}{r}\right) + A_{16}\left(v_{,x} + \frac{u_{,\theta}}{r}\right) \\
&\quad + \frac{B_{11}}{r}(u_{,x} - rw_{,xx} + r\gamma_{x,x}) + \frac{B_{12}}{r}\left(\frac{v_{,\theta}}{r} - \frac{w_{,\theta\theta}}{r} + \gamma_{\theta,\theta}\right) \\
&\quad + \frac{B_{16}}{r}(2v_{,x} - 2w_{,x\theta} + r\gamma_{\theta,x} + \gamma_{x,\theta}) \\
&\quad + \frac{D_{11}}{r^2}(-rw_{,xx} + r\gamma_{x,x}) + \frac{D_{16}}{r^2}(v_{,x} - w_{,x\theta} + r\gamma_{\theta,x})
\end{aligned} \tag{19a}$$

$$
\begin{aligned}
M_x &= \int_{-t/2}^{t/2} \sigma_x z\left(1+\frac{z}{r}\right)\mathrm{d}z \\
&= \int_{-t/2}^{t/2} (E_{11}\varepsilon_x + E_{12}\varepsilon_\theta + E_{16}\gamma_{x\theta}) z\left(1+\frac{z}{r}\right)\mathrm{d}z \\
&= B_{11}u_{,x} + B_{12}\left(\frac{v_{,\theta}}{r}+\frac{w}{r}\right) + B_{16}\left(v_{,x}+\frac{u_{,\theta}}{r}\right) \\
&\quad + \frac{D_{11}}{r}(u_{,x} - rw_{,xx} + r\gamma_{x,x}) + \frac{D_{12}}{r}\left(\frac{v_{,\theta}}{r} - \frac{w_{,\theta\theta}}{r} + \gamma_{\theta,\theta}\right) \\
&\quad + \frac{D_{16}}{r}(2v_{,x} - 2w_{,x\theta} + r\gamma_{\theta,x} + \gamma_{x,\theta})
\end{aligned} \tag{19b}
$$

$$
\begin{aligned}
M_{x\theta} &= \int_{-t/2}^{t/2} \tau_{x\theta} z\left(1+\frac{z}{r}\right)\mathrm{d}z \\
&= \int_{-t/2}^{t/2} (E_{16}\varepsilon_x + E_{26}\varepsilon_\theta + E_{66}\gamma_{x\theta}) z\left(1+\frac{z}{r}\right)\mathrm{d}z \\
&= B_{16}u_{,x} + B_{26}\left(\frac{v_{,\theta}}{r}+\frac{w}{r}\right) + B_{66}\left(v_{,x}+\frac{u_{,\theta}}{r}\right) \\
&\quad + \frac{D_{16}}{r}(u_{,x} - rw_{,xx} + r\gamma_{x,x}) + \frac{D_{26}}{r}\left(\frac{v_{,\theta}}{r} - \frac{w_{,\theta\theta}}{r} + \gamma_{\theta,\theta}\right) \\
&\quad + \frac{D_{66}}{r}(2v_{,x} - 2w_{,x\theta} + r\gamma_{\theta,x} + \gamma_{x,\theta})
\end{aligned} \tag{19c}
$$

A_{ij}, B_{ij}, D_{ij}, and S_{ij} are the stiffness coefficients of moderately thick anisotropic shells. They are given by

$$
\begin{aligned}
&\{A_{ij}, B_{ij}, D_{ij}\} = \int_{-t/2}^{t/2} E_{ij}\{1, z, z^2\}\,\mathrm{d}z \qquad (i,j = 1,2,6), \\
&k_{ij}S_{ij} = \int_{-t/2}^{t/2} G_{ij}\,\mathrm{d}z \qquad (i,j = 1,2)
\end{aligned} \tag{20}
$$

where repeated subindices do not imply summations. N_θ, $N_{\theta x}$, $N_{x\theta}$, M_θ, and $M_{\theta x}$ are obtained similarly. Substituting Eqs. (19) into Eqs. (16) then enables the partial differential equations of equilibrium to be expressed in terms of the displacements of the middle surface of the shell:

$$
\begin{bmatrix}
h_{11}-f_{11} & h_{12}-f_{12} & h_{13}-f_{13} & h_{14} & h_{15} \\
 & h_{22}-f_{22} & h_{23}-f_{23} & h_{24} & h_{25} \\
 & & h_{33}-f_{33} & h_{34} & h_{35} \\
 & \text{sym} & & h_{44} & h_{45} \\
 & & & & h_{55}
\end{bmatrix}
\begin{bmatrix} u \\ v \\ w \\ \gamma_x \\ \gamma_\theta \end{bmatrix}
= \begin{bmatrix} 0 \\ 0 \\ 0 \\ 0 \\ 0 \end{bmatrix} \tag{21}
$$

where

$$
\begin{aligned}
h_{11} &= (a_{11}+b_{11})r^2()_{,xx} + (2a_{16})r()_{,x\theta} + (a_{66}-b_{66}+d_{66})()_{,\theta\theta} \\
h_{12} &= (a_{16}+2b_{16}+d_{16})r^2()_{,xx} \\
&\quad + (a_{12}+a_{66}+b_{12}+b_{66})r()_{,x\theta} + a_{26}()_{,\theta\theta} \\
h_{13} &= a_{12}r()_{,x} + (a_{26}-b_{26}+d_{26})()_{,\theta} - (b_{11}+d_{11})r^3()_{,xxx} \\
&\quad + (-3b_{16}-d_{16})r^2()_{,xx\theta} - (b_{12}+2b_{66}-d_{66})r()_{,x\theta\theta} \\
&\quad - (b_{26}-d_{26})()_{,\theta\theta\theta} \\
h_{14} &= (b_{11}+d_{11})r^3()_{,xx} + 2b_{16}r^2()_{,x\theta} + (b_{66}-d_{66})r()_{,\theta\theta} \\
h_{15} &= (b_{16}+d_{16})r^3()_{,xx} + (b_{12}+b_{66})r^2()_{,x\theta} + (b_{26}-d_{26})r()_{,\theta\theta} \\
h_{22} &= (a_{66}+3b_{66}+3d_{66})r^2()_{,xx} + (2a_{26}+4b_{26}+2d_{26})r()_{,x\theta} \\
&\quad + (1+b_{22})()_{,\theta\theta}
\end{aligned}
$$

$$
\begin{aligned}
h_{23} &= (a_{26}+b_{26})r()_{,x} + ()_{,\theta} + (-b_{16}-2d_{16})r^3()_{,xxx} \\
&\quad + (-b_{12}-2b_{66}-d_{12}-3d_{66})r^2()_{,xx\theta} \\
&\quad + (-3b_{26}-2d_{26})r()_{,x\theta\theta} - b_{22}()_{,\theta\theta\theta} \\
h_{24} &= (b_{16}+2d_{16})r^3()_{,xx} \\
&\quad + (b_{12}+b_{66}+d_{12}+d_{66})r^2()_{,x\theta} + b_{26}r()_{,\theta\theta} \\
h_{25} &= (b_{66}+2d_{66})r^3()_{,xx} + 2(b_{26}+d_{26})r^2()_{,x\theta} + b_{22}r()_{,\theta\theta} \\
h_{33} &= (1-b_{22}+d_{22})() - 2b_{12}r^2()_{,xx} + (-4b_{26}+2d_{26})r()_{,x\theta} \\
&\quad + (-2b_{22}+2d_{22})()_{,\theta\theta} + d_{11}r^4()_{,xxxx} + 4d_{16}r^3()_{,xxx\theta} \\
&\quad + (2d_{12}+4d_{66})r^2()_{,xx\theta\theta} + 4d_{26}r()_{,x\theta\theta\theta} + d_{22}()_{,\theta\theta\theta\theta} \\
h_{34} &= b_{12}r^2()_{,x} + (b_{26}-d_{26})r()_{,\theta} - d_{11}r^4()_{,xxx} - 3d_{16}r^3()_{,xx\theta} \\
&\quad - (d_{12}+2d_{66})r^2()_{,x\theta\theta} - d_{26}r()_{,\theta\theta\theta} \\
h_{35} &= b_{26}r^2()_{,x} + (b_{22}-d_{22})r()_{,\theta} - d_{16}r^4()_{,xxx} \\
&\quad - (d_{12}+2d_{66})r^3()_{,xx\theta} - 3d_{26}r^2()_{,x\theta\theta} - d_{22}r()_{,\theta\theta\theta} \\
h_{44} &= -rs_{11}() + d_{11}r^3()_{,xx} + 2d_{16}r^2()_{,x\theta} + d_{66}r()_{,\theta\theta} \\
h_{45} &= -rs_{12}() + d_{16}r^3()_{,xx} + (d_{12}+d_{66})r^2()_{,x\theta} + d_{26}r()_{,\theta\theta} \\
h_{55} &= -rs_{22}() + d_{66}r^3()_{,xx} + 2d_{26}r^2()_{,x\theta} + d_{22}r()_{,\theta\theta}
\end{aligned} \tag{22a}
$$

$$
\begin{aligned}
f_{11} &= q_2 r^2()_{,xx} + 2q_3 r()_{,x\theta} \\
f_{12} &= 0 \\
f_{13} &= 0 \\
f_{22} &= q_2 r^2()_{,xx} + 2q_3 r()_{,x\theta} \\
f_{23} &= 2q_3 r()_{,x} \\
f_{33} &= -q_2 r^2()_{,xx} - 2q_3 r()_{,x\theta}
\end{aligned} \tag{22b}
$$

where

$$
\begin{aligned}
&\{a_{ij}, b_{ij}, d_{ij}\} = (1/A_{22})\{A_{ij}, B_{ij}/r, D_{ij}/r^2\} \qquad (i,j = 1,2,6), \\
&s_{ij} = (1/A_{22})k_{ij}S_{ij} \qquad (i,j = 1,2), \qquad \{q_2, q_3\} = (1/A_{22})\{P, T\}
\end{aligned} \tag{23}
$$

and where repeated subindices do not imply summations. By neglecting those terms containing γ_x and γ_θ, we can confirm that the matrix Eq. (21) can be reduced to the Flügge equations extended by Cheng and Ho [9] for anisotropic circular cylindrical shells.

IV. Solution of Differential Equations

For solving Eq. (21), let the displacements of the middle surface of the shell be

$$
\begin{aligned}
u &= U\sin(\lambda x/r + n\theta) \\
v &= V\sin(\lambda x/r + n\theta) \\
w &= W\cos(\lambda x/r + n\theta) \\
\gamma_x &= (\Gamma_x/r)\sin(\lambda x/r + n\theta) \\
\gamma_\theta &= (\Gamma_\theta/r)\sin(\lambda x/r + n\theta)
\end{aligned} \tag{24}
$$

where U, V, W, Γ_x, and Γ_θ are constants; $\lambda = m\pi r/l$, n is the number of waves in the circumferential direction; and m is the number of half-waves in the axial direction if the circumferential waves do not spin along the circular cylindrical shell. We can easily confirm that Eqs. (24) satisfy the differential equations.

Substituting Eqs. (24) in Eqs. (21), one gets

$$\begin{bmatrix} k_{11}+g_{11} & k_{12}+g_{12} & k_{13}+g_{13} & k_{14} & k_{15} \\ & k_{22}+g_{22} & k_{23}+g_{23} & k_{24} & k_{25} \\ & & k_{33}+g_{33} & k_{34} & k_{35} \\ & \text{sym} & & k_{44} & k_{45} \\ & & & & k_{55} \end{bmatrix} \begin{bmatrix} U \\ V \\ W \\ \Gamma_x \\ \Gamma_\theta \end{bmatrix}$$

$$= [K+G] \begin{bmatrix} U \\ V \\ W \\ \Gamma_x \\ \Gamma_\theta \end{bmatrix} = \begin{bmatrix} 0 \\ 0 \\ 0 \\ 0 \\ 0 \end{bmatrix} \tag{25}$$

where

$$\begin{aligned}
k_{11} &= (a_{11}+b_{11})\lambda^2 + 2na_{16}\lambda + n^2(a_{66}-b_{66}+d_{66}) \\
k_{12} &= (a_{16}+2b_{16}+d_{16})\lambda^2 + n(a_{12}+a_{66}+b_{12}+b_{66})\lambda + n^2a_{26} \\
k_{13} &= (b_{11}+d_{11})\lambda^3 + n(3b_{16}+d_{16})\lambda^2 \\
&\quad + [n^2(b_{12}+2b_{66}-d_{66})+a_{12}]\lambda + n^3(b_{26}-d_{26}) \\
&\quad + n(a_{26}-b_{26}+d_{26}) \\
k_{14} &= (b_{11}+d_{11})\lambda^2 + 2nb_{16}\lambda + n^2(b_{66}-d_{66}) \\
k_{15} &= (b_{16}+d_{16})\lambda^2 + n(b_{12}+b_{66})\lambda + n^2(b_{26}-d_{26}) \\
k_{22} &= (a_{66}+3b_{66}+3d_{66})\lambda^2 + 2n(a_{26}+2b_{26}+d_{26})\lambda \\
&\quad + n^2(1+b_{22}) \\
k_{23} &= (b_{16}+2d_{16})\lambda^3 + n(b_{12}+2b_{66}+d_{12}+3d_{66})\lambda^2 \\
&\quad + [n^2(3b_{26}+2d_{26})+a_{26}+b_{26}]\lambda + n^3b_{22} + n \\
k_{24} &= (b_{16}+2d_{16})\lambda^2 + n(b_{12}+b_{66}+d_{12}+d_{66})\lambda + n^2b_{26} \\
k_{25} &= (b_{66}+2d_{66})\lambda^2 + 2n(b_{26}+d_{26})\lambda + n^2b_{22} \\
k_{33} &= d_{11}\lambda^4 + 4nd_{16}\lambda^3 + 2[n^2(d_{12}+2d_{66})+b_{12}]\lambda^2 \\
&\quad + 2n(2n^2d_{26}+2b_{26}-d_{26})\lambda + (n^2-1)^2d_{22} \\
&\quad + (2n^2-1)b_{22} + 1 \\
k_{34} &= d_{11}\lambda^3 + 3nd_{16}\lambda^2 + [n^2(d_{12}+2d_{66})+b_{12}]\lambda \\
&\quad + n[b_{26}+(n^2-1)d_{26}] \\
k_{35} &= d_{16}\lambda^3 + n(d_{12}+2d_{66})\lambda^2 + (b_{26}+3n^2d_{26})\lambda \\
&\quad + n[b_{22}+(n^2-1)d_{22}] \\
k_{44} &= d_{11}\lambda^2 + 2nd_{16}\lambda + n^2d_{66} + s_{11} \\
k_{45} &= d_{16}\lambda^2 + n(d_{12}+d_{66})\lambda + n^2d_{26} + s_{12} \\
k_{55} &= d_{66}\lambda^2 + 2nd_{26}\lambda + n^2d_{22} + s_{22}
\end{aligned} \tag{26a}$$

$$\begin{aligned}
g_{11} &= -q_2\lambda^2 - 2nq_3\lambda \\
g_{12} &= 0 \\
g_{13} &= 0 \\
g_{22} &= -q_2\lambda^2 - 2nq_3\lambda \\
g_{23} &= -2q_3\lambda \\
g_{33} &= -q_2\lambda^2 - 2nq_3\lambda
\end{aligned} \tag{26b}$$

If the solutions of Eq. (25) are to be nontrivial, the determinant of the coefficient matrix must be equal to zero:

$$|[K]+[G]| = 0 \tag{27}$$

Equation (27) is expanded as a tenth-degree polynomial of λ for which the ten roots can be found by substituting q_2, q_3, n, and the given dimensions and material properties into it; $(U/W)_i$, $(V/W)_i$, $(\Gamma_x/W)_i$, and $(\Gamma_\theta/W)_i$ for each λ_i can be determined in terms of W_i from Eqs. (25).

By the principle of superposition, Eqs. (24) become

$$\begin{aligned}
u &= \sum_{i=1}^{10} (U/W)_i W_i \sin(\lambda_i x/r + n\theta) \\
v &= \sum_{i=1}^{10} (V/W)_i W_i \sin(\lambda_i x/r + n\theta) \\
w &= \sum_{i=1}^{10} W_i \cos(\lambda_i x/r + n\theta) \\
\gamma_x &= \sum_{i=1}^{10} (\Gamma_x/W)_i W_i \sin(\lambda_i x/r + n\theta) \\
\gamma_\theta &= \sum_{i=1}^{10} (\Gamma_\theta/W)_i W_i \sin(\lambda_i x/r + n\theta)
\end{aligned} \tag{28}$$

Substituting Eqs. (28) into Eqs. (17), one obtains ten homogeneous equations of ten unknown W_i. For example, the simply supported condition $v = w = N_x = M_x = M_{x\theta} = 0$ becomes

$$\begin{aligned}
v &= \sum_{i=1}^{10} [(V/W)_i W_i \sin(\lambda_i x/r)\cos(n\theta) \\
&\quad + (V/W)_i W_i \cos(\lambda_i x/r)\sin(n\theta)] = 0 \\
w &= \sum_{i=1}^{10} [W_i \cos(\lambda_i x/r)\cos(n\theta) - W_i \sin(\lambda_i x/r)\sin(n\theta)] = 0 \\
N_x &= \sum_{i=1}^{10} [(N_x/W)_i W_i \sin(\lambda_i x/r)\cos(n\theta) \\
&\quad + (N_x/W)_i W_i \cos(\lambda_i x/r)\sin(n\theta)] = 0 \\
M_x &= \sum_{i=1}^{10} [(M_x/W)_i W_i \sin(\lambda_i x/r)\cos(n\theta) \\
&\quad + (M_x/W)_i W_i \cos(\lambda_i x/r)\sin(n\theta)] = 0 \\
M_{x\theta} &= \sum_{i=1}^{10} [(M_{x\theta}/W)_i W_i \sin(\lambda_i x/r)\cos(n\theta) \\
&\quad + (M_{x\theta}/W)_i W_i \cos(\lambda_i x/r)\sin(n\theta)] = 0
\end{aligned} \tag{29}$$

where $(N_x/W)_i$, $(M_x/W)_i$, and $(M_{x\theta}/W)_i$ are obtained by substituting Eqs. (28) into Eqs. (19) as follows:

$$\begin{aligned}
(N_x/W)_i &= A_{22} r[(U/W)_i\{a_{16}n + (a_{11}+b_{11})\lambda_i\} \\
&\quad + (V/W)_i\{(a_{12}+b_{12})n + (a_{16}+2b_{16}+d_{16})\lambda_i\} \\
&\quad + W_i\{a_{12}+b_{12}n^2 + (2b_{16}+d_{16})n\lambda_i + (b_{11}+d_{11})\lambda_i^2\} \\
&\quad + (\Gamma_{xz}/W)_i\{b_{16}n + (b_{11}+d_{11})\lambda_i\} \\
&\quad + (\Gamma_{\theta z}/W)_i\{b_{12}n + (b_{16}+d_{16})\lambda_i\}] \\
(M_x/W)_i &= A_{22}[(U/W)_i\{b_{16}n + (b_{11}+d_{11})\lambda_i\} \\
&\quad + (V/W)_k\{(b_{12}+d_{12})n + (b_{16}+2d_{16})\lambda_i\} \\
&\quad + W_i\{b_{12}+d_{12}n^2 + 2d_{16}n\lambda_i + d_{11}\lambda_i^2\} \\
&\quad + (\Gamma_{xz}/W)_i(d_{16}n + d_{11}\lambda_i) + (\Gamma_{\theta z}/W)_i(d_{12}n + d_{16}\lambda_i)] \\
(M_{x\theta}/W)_i &= A_{22}[(U/W)_i\{b_{66}n + (b_{16}+d_{16})\lambda_i\} \\
&\quad + (V/W)_i\{(b_{26}+d_{26})n + (b_{66}+2d_{66})\lambda_i\} \\
&\quad + W_i(b_{26}+d_{26}n^2 + 2d_{66}n\lambda_i + d_{16}\lambda_i^2) \\
&\quad + (\Gamma_{xz}/W)_i(d_{66}n + d_{16}\lambda_i) + (\Gamma_{\theta z}W)_i(d_{26}n + d_{66}\lambda_i)]
\end{aligned} \tag{30}$$

Because Eqs. (29) must be equal to zero at $x = l/2$ and every θ, we have

$$\begin{aligned}
&\sum_{i=1}^{10}[(V/W)_i W_i \sin(\lambda_i x/r)] = 0\\
&\sum_{i=1}^{10}[(V/W)_i W_i \cos(\lambda_i x/r)] = 0\\
&\sum_{i=1}^{10}[W_i \cos(\lambda_i x/r)] = 0\\
&\sum_{i=1}^{10}[W_i \sin(\lambda_i x/r)] = 0\\
&\sum_{i=1}^{10}[(N_x/W)_i W_i \sin(\lambda_i x/r)] = 0\\
&\sum_{i=1}^{10}[(N_x/W)_i W_i \cos(\lambda_i x/r)] = 0\\
&\sum_{i=1}^{10}[(M_x/W)_i W_i \sin(\lambda_i x/r)] = 0\\
&\sum_{i=1}^{10}[(M_x/W)_i W_i \cos(\lambda_i x/r)] = 0\\
&\sum_{i=1}^{10}[(M_{x\theta}/W)_i W_i \sin(\lambda_i x/r)] = 0\\
&\sum_{i=1}^{10}[(M_{x\theta}/W)_i W_i \cos(\lambda_i x/r)] = 0
\end{aligned} \tag{31}$$

Equations for other boundary conditions can be formulated similarly. If the solutions of Eqs. (31) are to be nontrivial, the determinant of the coefficients Δ must equal zero. The determinant Δ can be written

$$\Delta\begin{pmatrix} L, r, a_{ij}, b_{ij}, d_{ij}, n, q_2, q_3 \\ \lambda_i(r, a_{ij}, b_{ij}, d_{ij}, n, q_2, q_3) \end{pmatrix} = 0 \tag{32}$$

When Eq. (32) is equal to zero, the boundary conditions are satisfied. Thus, Eqs. (28) satisfy both the partial differential equations and the boundary conditions. When the material and dimensions are given, Eq. (32) depends on only n, q_2, and q_3. The load parameters q_2 and q_3 still depend on the wave number n, and so the wave number n must be varied systematically to find the minimum load parameters q_2 and q_3.

When $n = 1$, the determinant Eqs. (27) have double roots at $\lambda = 0$. In this case, Eqs. (28) become

$$\begin{aligned}
u &= \sum_{i=1}^{8}(U/W)_i W_i \sin(\lambda_i x/r + n\theta) - W_9 \sin(n\theta)\\
v &= \sum_{i=1}^{8}(V/W)_i W_i \sin(\lambda_i x/r + n\theta)\\
&\quad + W_9 x/r \cos(n\theta) - W_{10} \sin(n\theta)\\
w &= \sum_{i=1}^{8} W_i \cos(\lambda_i x/r + n\theta)\\
&\quad + W_9 x/r \sin(n\theta) + W_{10} \cos(n\theta)\\
\gamma_x &= \sum_{i=1}^{8}(\Gamma_x/W)_i W_i \sin(\lambda_i x/r + n\theta)\\
\gamma_\theta &= \sum_{i=1}^{8}(\Gamma_\theta/W)_i W_i \sin(\lambda_i x/r + n\theta)
\end{aligned} \tag{33}$$

Equations (29–32) for $n = 1$ can be formulated similarly.

V. Some Examples and Validation

To verify the analytical model, numerical examples shall be compared with established analyses. In this paper, only axial compression buckling is discussed. Buckling under the combined load of torsion and axial compression will be discussed in another paper.

Material properties of the CFRP prepreg and the honeycomb core, which are used in this numerical calculation, are listed in Table 1, and the layups treated in this paper are listed in Table 2.

A. Effect of Transverse Shear Deformation

The calculation was performed using Eq. (32) to investigate the effect of transverse shear stiffness on the buckling load. For comparison with the Stein and Mayers solution [12], the simply supported condition $v = w = N_x = M_x = M_{x\theta} = 0$ was used. The shells of the cylinders analyzed are made of laminated CFRP and of CFRP-honeycomb sandwich. The effect of transverse shear stiffness was investigated by using two different transverse shear stiffness values, one calculated from the material properties and the other almost infinite. The buckling loads were calculated over a wide range of lengths.

The normalized axial load factor is defined as follows:

$$K_c = P/N_{xcr0} \tag{34}$$

where

$$N_{xcr0} = 2/r\sqrt{D_{11}A_{22}} \tag{35}$$

Equation (35) is almost equal to the buckling load for orthotropic circular cylindrical shells [21], which is

$$2/r\sqrt{D_{11}A_{22}(1 - \nu_1\nu_2)} \tag{36}$$

Equation (36) is based on Donnell's equation. Note that for isotropic material, Eq. (36) is reduced to

$$N_{xcr0} = \frac{Et^2}{\sqrt{3(1-\nu^2)}r} \tag{37}$$

Equation (37) is a well-known equation for the buckling load of an isotropic circular cylindrical shell.

The results for circular cylindrical shells that have a radius of 597 mm and are made of laminated CFRP that is 3 mm thick ($r/t = 199$) and 9.95 mm thick ($r/t = 60$) are shown in Figs. 3a and 3b. The layup analyzed was layup B, but two different values of transverse shear stiffness were used: $G_{11} = G_{22} = 4000$ MPa and $G_{11} = G_{22} = 4 \times 10^7$ MPa, which can be regarded as infinite. In each case, $G_{12} = 0$. Shear correction factors $k_{11} = k_{22} = 5/6$ were used. The solution is expected to come close to the Euler buckling load when l/r is large and to come close to the buckling load of a plane plate strip when l/r is small [19]. Hence, for comparison with the Euler buckling load, the load factor K_c is plotted against $(l/r)/\sqrt{r/t}$ in Fig. 3a. And for comparison with the buckling load of a plane plate strip, K_c is plotted against $(l/r) \times \sqrt{r/t}$ in Fig. 3b.

As shown in Fig. 3a, results obtained when including the effect of transverse shear deformation are lower than those obtained when not

Table 1 Material properties

Property	Value
CFRP	
E_{11}	380,000 MPa
E_{22}	6000 MPa
G_{12}	4000 MPa
υ_{12}	0.33
Honeycomb core	
$G_{44} = G_{55}$	120 MPa
G_{45}	0

Table 2 Layup specifications[a]

Layup	Shell type	Comments	Layup sequence
A	Honeycomb sandwich	$D_{11} = 3.80 \times 10^6$ Nmm, $A_{22} = 1.34 \times 10^5$ N/mm	$[0/60/-60/\text{honeycomb}]_s$
B	Laminate	$D_{16} = D_{26} = 1260$ Nmm	$[-45/45/0/90/90/45/0/0/90/-45]_s$
C	Laminate	$D_{16} = D_{26} = 101,000$ Nmm	$[45/45/0/90/90/0/90/0/-45/-45]_s$
D	Laminate	$B_{16} = B_{26} = 67,400$ N	$[45/45/0/90/90/0/90/0/-45/-45]_{as}$
E	Laminate	All couplings are included	$[90/45/0/45/0/0/0/0/-45/-45/90/90/90/90/90/45/45/-45/45/45]$

[a]The top layer is the leftmost layer; *s* indicates a symmetric layup, and as indicates an antisymmetric layup.

including it. For $(l/r)/\sqrt{r/t}$ between 0.03 and 0.5, the K_c for the $r/t = 60$ shell calculated including the effect of transverse shear deformation is 1–13% lower than the K_c calculated neglecting it. These differences are not negligible.

The curves in Fig. 3a fluctuate when $(l/r)/\sqrt{r/t}$ is large. This fluctuation is caused by the number of half-waves in the axial direction. Similar fluctuating curves for isotropic materials are shown in Flügge's text [19] and can be seen in Fig. 4 in this paper.

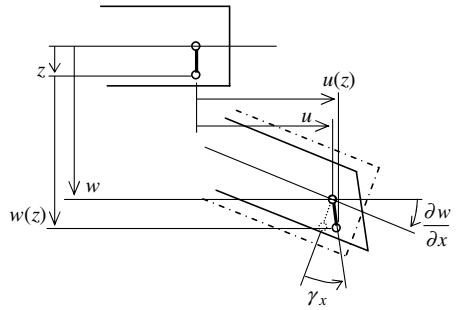

Fig. 2 Deformation of shell section.

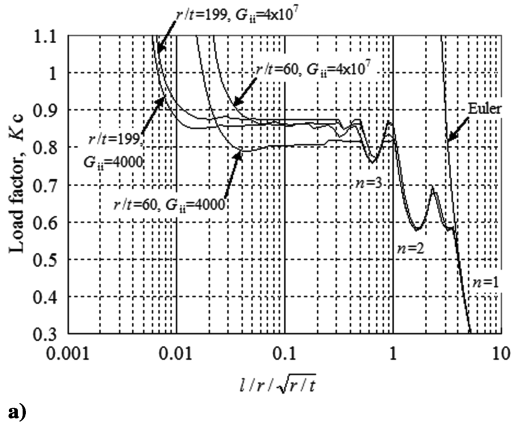

a)

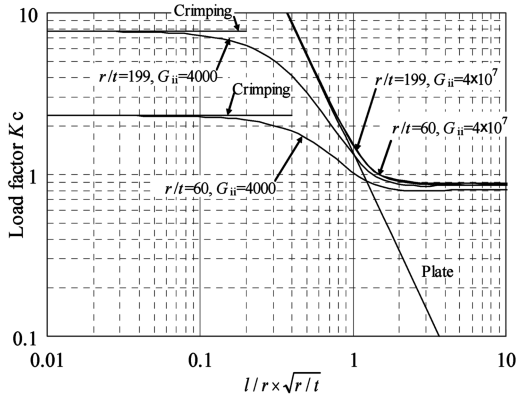

b)

Fig. 3 Laminated CFRP cylindrical shell.

On the right-hand side of Fig. 3a, the curve for $n = 1$ comes remarkably close to the Euler buckling load for a tube:

$$2\pi r \cdot P = \pi^2 \frac{A_{11}^* \cdot \pi r^3}{l^2} \tag{38}$$

Thus, this solution can be applied for long cylindrical shells.

In Fig. 3b, the curves calculated without effect of transverse shear deformation come close to the buckling load of a plane plate strip:

$$P = \frac{D_{11} \cdot \pi^2}{l^2} \tag{39}$$

On the other hand, when $(l/r) \times \sqrt{r/t}$ is small, the curves calculated with the effect of transverse shear deformation are considerably lower than those calculated without it.

According to Stein and Mayers [12], when the transverse shear stiffness is small, the buckling load becomes

$$P = k_{ii} S_{ii} \tag{40}$$

where $k_{11}S_{11} = k_{22}S_{22} = k_{ii}S_{ii}$ and $k_{12}S_{12} = 0$. The buckling mode is called "crimping." The load factors of crimping are shown on the left-hand side of Fig. 3b. Each curve including the effect of transverse shear deformation comes close to each crimping load factor. Thus, it is concluded that the reduction is appropriate and is caused by crimping.

The results calculated for a CFRP-honeycomb-sandwich circular cylindrical shell with a radius of 833 mm, a CFRP skin 0.45 mm thick, and a honeycomb core 10 mm thick are shown in Fig. 4. The layup analyzed was layup A, which has a honeycomb core between two CFRP face sheets. Two values of transverse shear stiffness were used: $k_{11}S_{11} = k_{22}S_{22} = 1000$ N/mm, which was calculated from the honeycomb core's plate shear modulus, and $k_{11}S_{11} = k_{22}S_{22} = 10^7$ N/mm, which can be regarded as almost infinite. Again, $k_{12}S_{12} = 0$ was used for each case.

One can see in Fig. 4 that when $l/r < 9$, the buckling load calculated with the effect of transverse shear deformation, 0.584 and almost constant, is much smaller than that calculated without it. The difference between the buckling loads calculated with and without the transverse shear deformation is larger than that in the case of the laminated CFRP circular cylindrical shell.

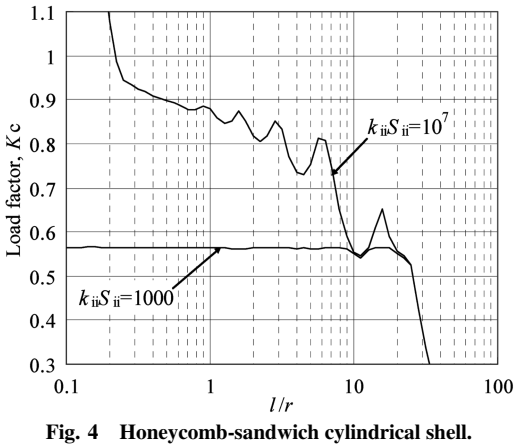

Fig. 4 Honeycomb-sandwich cylindrical shell.

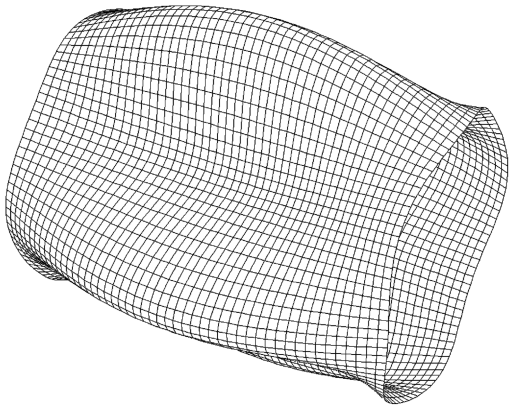

$k_{ib}S_{ii}=10^7$ N/mm

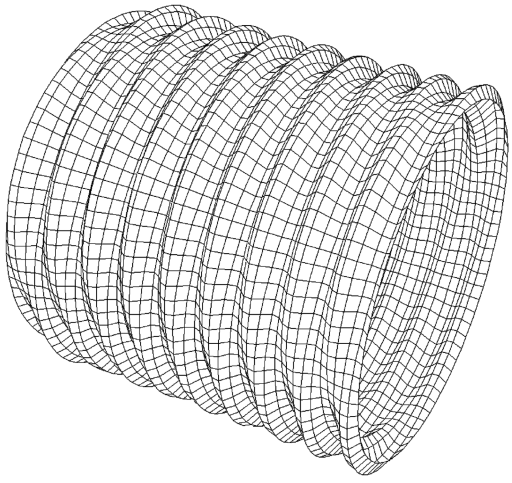

$k_{ib}S_{ii}=1000$ N/mm

Fig. 5 Effect of transverse shear deformation: Change in buckling mode.

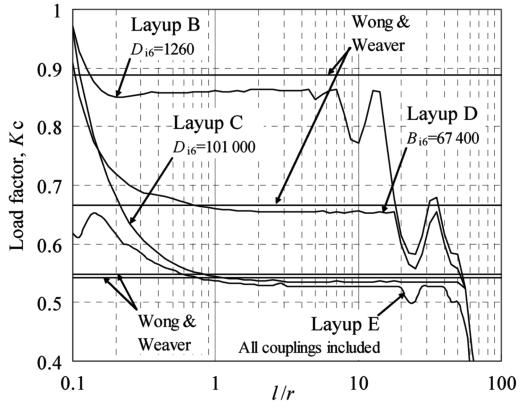

Fig. 6 Effect of coupling stiffness. Wong and Weaver results are calculated using Eq. (12) in [7].

The buckling modes of CFRP-honeycomb-sandwich circular cylindrical shells with $l/r = 2$ are shown in Fig. 5. When transverse shear stiffness is high, the buckling mode becomes the thin circular cylindrical shell's buckling mode as shown. But when transverse shear stiffness is small, the small buckling wave appears in an axial direction. The mode shape is that of the typical crimping mode.

When $k_{11}S_{11} = k_{22}S_{22} = 1000$ N/mm, axial buckling load factor which is obtained using the Stein and Mayers solution is

$$K_c = k_{11}S_{11}/(2/r\sqrt{D_{11}A_{22}}) = 1000/(2/833\sqrt{3.80\times10^6\times1.34\times10^5}) = 0.584 \quad (41)$$

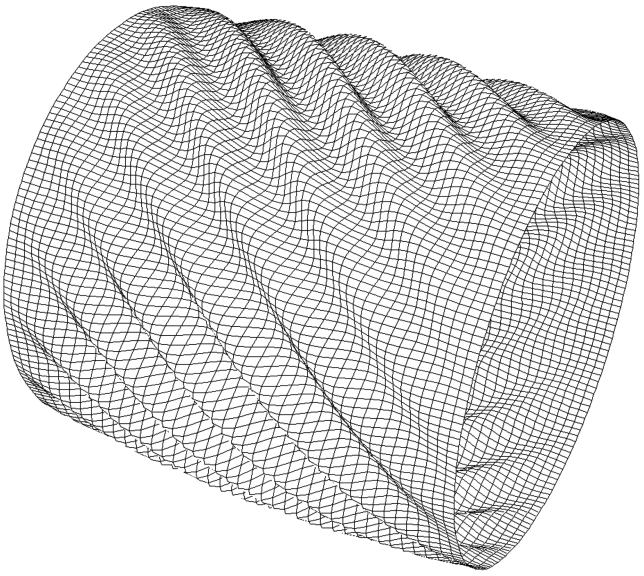

Fig. 7 Effect of coupling stiffness: spiral mode (layup C).

This value matches the value in the region $l/r < 9$ in Fig. 4. And note that the Stein and Mayers [12] solution is based on Donnell's [8] theory, which cannot be applied to long cylindrical shells. So it is natural that the Stein and Mayers [12] solution is larger than the present solution in the $l/r > 9$ region in Fig. 4.

B. Effect of Coupling Stiffness

Another parametric study was done using Eq. (32) to investigate the effect of coupling stiffness on the buckling load. For comparison with the Wong and Weaver prediction [7], the simply supported condition $v = w = N_x = M_x = M_{x\theta} = 0$ was used. The dimensions of the circular cylindrical shells were a radius of 597 mm and a thickness of 3 mm. The layups analyzed were B, C, D, and E, which are listed in Table 2. In the layups B, C, and D, the A matrices are equal, each B_{11}, B_{12}, B_{22}, and B_{66} is zero, and each D_{11}, D_{12}, D_{22}, and D_{66} is almost equal. However, as shown in Table 2, the flexural/twist couplings D_{16}, D_{26} and extension/twist couplings B_{16}, and B_{26} are very different. The differences are caused by the layup sequence of ±45 deg layers. Layup E has all the coupling stiffnesses because it is an asymmetric layup. The numerical results using Eq. (32) and the corresponding results calculated using Eq. (12) in [7] are shown in Fig. 6. The results were normalized by the Eq. (35) result calculated using A_{22} and D_{11} of layup B.

It is clear from Fig. 6 that the influence of the coupling stiffness is considerably large on the whole range of l/r and that large coupling stiffness reduces the buckling load. This tendency is the same as that in the results of Wong and Weaver [7]. Note that Wong and Weaver's solution is also based on Donnell's [8] theory, which is independent of the length of the cylindrical shell, and thus their solution has a discrepancy in the region of $l/r < 1$ and $l/r > 7$ in Fig. 6.

The results calculated using Eq. (32) are compared in Table 3 with the corresponding results calculated using Eq. (12) in [7]. The ratio of length to radius is 2.0. It is evident that the predictions made using Eq. (32) are within about 3% of those made using Wong and Weaver's [7] solution.

On the other hand, from a practical viewpoint, it is important that in spite of layup C being symmetric, the buckling load of layup C is

Table 3 Predicted buckling load factors for cylindrical shells with $l/r = 2.0$

Layup	Present	Wong and Weaver [7]	Difference, %
B	0.862	0.881	−2.1
C	0.537	0.542	−1.0
D	0.655	0.667	−1.8
E	0.530	0.537	−1.4

much smaller than that of layup B. Thus, it is not sufficient to simply use a symmetric layup. Designers should use a layup that has small flexural/twist coupling.

The buckling mode of layup C at $l/r = 2.0$ that was obtained using Eq. (28) is shown in Fig. 7, in which one sees the typical spiral mode caused by flexural/twist coupling. Wong and Weaver [7] obtained a similar spiral mode with the finite element analysis.

VI. Conclusions

An analysis of the linear buckling of moderately thick and anisotropic circular cylindrical shells under axial load was developed by extending Flügge's equations. This analysis also satisfies boundary condition and was verified by comparing its predictions with those of established analyses. The effects of axial compression and torsion will be discussed in another paper.

References

[1] Hedgepeth, J. M., and Hall, D. B., "Stability of Stiffened Cylinders," *AIAA Journal*, Vol. 3, No. 12, 1965, pp. 2275–2287.

[2] Tasi, J., "Effect of Heterogeneity on the Stability of Composite Cylindrical Shells Under Axial Compression," *AIAA Journal*, Vol. 4, No. 6, 1966, pp. 1058–1062.

[3] Jones, R. M., "Buckling of Circular Cylindrical Shells with Multiple Orthotropic Layers and Eccentric Stiffeners," *AIAA Journal*, Vol. 6, No. 12, 1968, pp. 2301–2305.

[4] Soong, T. C., "Buckling of Cylindrical Shells with Eccentric Spiral-Type Stiffeners," *AIAA Journal*, Vol. 7, No. 1, 1969, pp. 65–72.

[5] Onoda, J., "Optimal Laminate Configurations of Cylindrical Shells for Axial Buckling," *AIAA Journal*, Vol. 23, No. 7, 1985, pp. 1093–1098.

[6] Weaver, P. M., "Anisotropy-Induced Spiral Buckling in Compression-Loaded Cylindrical Shells," *AIAA Journal*, Vol. 40, No. 5, 2002, pp. 1001–1007.

[7] Wong, K. F. W., and Weaver, P. M., "Approximate Solution for the Compression Buckling of Fully Anisotropic Cylindrical Shells," *AIAA Journal*, Vol. 43, No. 12, 2005, pp. 2639–2645.

[8] Donnell, L. H., "Stability of Thin-Walled Tube under Torsion," NACA, Rept. 479, 1933, pp. 95–116.

[9] Cheng, S., and Ho, B. P. C., "Stability of Heterogeneous Aeolotropic Cylindrical Shells Under Combined Loading," *AIAA Journal*, Vol. 1, No. 4, 1963, pp. 892–898.

[10] Ho, B. P. C., and, Cheng, S., "Some Problems in Stability of Heterogeneous Aeolotropic Cylindrical Shells Under Combined Loading," *AIAA Journal*, Vol. 1, No. 7, 1963, pp. 1603–1607.

[11] Bert, C. W., and Kim, C. D., "Analysis of Buckling of Hollow Laminated Composite Drive Shafts," *Composites Science and Technology*, Vol 53, No. 3, 1995, pp. 343–351. doi:10.1016/0266-3538(95)00006-2

[12] Stein, M., and Mayers, J., "Compressive Buckling of Simply Supported Curved Plates and Cylindrical Shells of Sandwich Construction," NACA TN 2601, Jan. 1952.

[13] Geier, B., and Singh, G., "Some Simple Solutions for Buckling Loads of Thin and Moderately Thick Cylindrical Shells and Panels Made of Laminated Composite Material," *Aerospace Science and Technology*, Vol. 1, No. 1, pp. 47–63. doi:10.1016/S1270-9638(97)90023-7, 1997.

[14] Resse, C. D., and Bert, C. W., "Buckling of Orthotropic Sandwich Cylinders Under Axial Compression and Bending," *Journal of Aircraft*, Vol. 11, No. 4, 1974, pp. 207–212.

[15] Kardomateas, G. A., and Philobos, M. S., "Buckling of Thick Orthotropic Cylindrical Shells Under Combined External Pressure and Axial Compression," *AIAA Journal*, Vol. 33, No. 10, 1995, pp. 1946–1953.

[16] Love, A. E. H., *A Treatise on the Mathematical Theory of Elasticity*, 4th ed., Dover, New York, 1944, Chaps. 24 and 24A.

[17] Timoshenko, S., and Gere, J. M., *Theory of Elastic Stability*, 2nd ed., McGraw–Hill, New York, 1961, Chap. 11.

[18] Sanders. J. L., "An Improved First-Approximation Theory for Thin Shells," NASA TR-R-24, June 1959.

[19] Flügge, W., *Stresses in Shells*, 2nd ed., Springer–Verlag, New York, 1973, Chap. 8.

[20] Washizu, K., *Variational Methods in Elasticity & Plasticity*, 3rd ed., Pergamon, New York, 1982, Chaps. 3, and 4.

[21] *Handbook of Structural Stability*, Pt. 4, edited by Column Research Committee of Japan, Corona, Tokyo, 1971, p. 103.

F. Pai
Associate Editor